Article

Galectin-3 as TREM2 upstream factor contributes to lung ischemia-reperfusion injury by regulating macrophage polarization

Hao Liu, Lu Zhang, Zhen Liu, ..., Chen Zhao, Youyuan Guo, Fei Lin

linfei@gxmu.edu.cn

Highlights

Gal3 and TREM2 co-locate in macrophages

Inhibition of Gal3 recovers the downregulation of TREM2 in LIRI models

Inhibition of Gal3 and excitation of TREM2 can reduce LIRI lung injury

Article

Galectin-3 as TREM2 upstream factor contributes to lung ischemia-reperfusion injury by regulating macrophage polarization

Hao Liu,[1,2,3,4,5] Lu Zhang,[1,2,3,4,5] Zhen Liu,[1,2,3,4] Jinyuan Lin,[1,2,3,4] Xiaojing He,[1,2,3,4] Siyi Wu,[1,2,3,4] Yi Qin,[1,2,3,4] Chen Zhao,[1,2,3,4] Youyuan Guo,[1,2,3,4] and Fei Lin[1,2,3,4,6,*]

SUMMARY

Lung ischemia-reperfusion injury (LIRI) is a complex "aseptic" inflammatory response, macrophage play a pivotal role in the pathogenesis of LIRI. Galectin-3 (Gal3), a lectin implicated inflammation, has received limited attention in LIRI. Studies have reported Gal3 as a ligand for triggering receptor expressed on myeloid cell 2 (TREM2) in macrophages in Alzheimer's disease. Hence, we established LIRI C57BL/6 mice model and hypoxia/glucose deprivation and reoxygenation (OGD/R) model to investigate the relationship among Gal3, TREM2, and macrophage polarization. Our result demonstrated inhibition of Gal3 significantly reduced M1-type macrophage polarization while markedly increased M2-type in LIRI. In addition, we observed colocalization of Gal3 and TREM2 in macrophages, inhibition of Gal3 could recover the downregulation of TREM2 induced by LIRI while promoting TREM2 expression could attenuate lung injury in LIRI. In summary, our findings suggest Gal3 as an upstream factor of TREM2, play a crucial role in LIRI by regulating macrophage polarization.

INTRODUCTION

Lung ischemia-reperfusion injury (LIRI) is a multifaceted pathophysiological process characterized by an intense inflammatory, alveolar damage, and increased microvascular permeability.[1] The primary pathological mechanisms of LIRI involve inflammatory activation, dysregulation of pro- and anti-inflammatory cytokines,[2] with LIRI being a major factor contributor to the development of acute lung injury (ALI) or acute respiratory distress syndrome (ARDS).[3] However, the precise molecular mechanisms underlying LIRI remains elusive and effective prevention and treatment measures are still lacking.

Macrophages play a pivotal role in the pathogenesis of LIRI, and mounting evidences suggests that they are the key drivers of ALI.[4,5] Macrophage polarization refers to the ability of mature macrophages to undergo different phenotypic and functional divisions induced by various factors. This process can be broadly classified in two main groups: classically activated phenotype (M1-type) and alternatively activated phenotype (M2-type).[6] M1-type macrophages are characterized by their pro-inflammatory properties, which include high levels of pro-inflammatory cytokine production and the ability to facilitate immunity against foreign pathogens and tumor cells. In contrast M2-type macrophages possess anti-inflammatory and tissue repair properties as well as immunomodulatory functions.[7,8] The M1/M2 phenotype is distinguished by differential surface receptor expression, secretory profiles and functions.[9] The balance between the M1 and M2 phenotype determines organ fate in inflammation or injury. Macrophage polarization has been identified as a key coordinator in the pathogenesis of ALI.[10] Regulating macrophage polarization may alleviate lung injury caused by LIRI and provide a new treatment approach.

Galectin-3 (Gal3) is a member of the galactose lectin family, which exhibits ubiquitous expression in human tissues, including all types of immune cells (monocytes, macrophages, dendritic cells [DCs], neutrophils, etc.), fibroblasts, epithelial cells, and endothelial cells.[11,12] At the cellular level, Gal3 is primarily located in the cytoplasm. However, it can also be detected in the nucleus and secreted into both the cell surface and extracellular environment. Its function varies depending on its location.[13,14] Gal3 plays a crucial role in apoptosis, angiogenesis, inflammation, fibrosis, and host defense.[15] Previous studies on Gal3 mostly focused on cardiovascular and fibrosis,[16,17] but few studies on lung diseases. In recent years, Gal3 has

emerged as a new inflammatory factor that promotes inflammation by promoting host inflammatory response and regulating macrophages production of pro-inflammatory cytokines.[18,19] A study has demonstrated that inhibition of Gal3 attenuates LPS-induced ALI.[20]

Triggering receptor expressed on myeloid cells 2 (TREM2) is a transmembrane glycoprotein receptor that belongs to the immunoglobulin superfamily and is widely expressed on the surface of mononuclear phagocytes such as macrophages and microglia.[21] TREM2 has a diverse range of functions and is generally considered to be a negative regulator of the immune response, attenuating inflammatory responses in multiple cell lines. In recent years, extensive research has focused on TREM2 in the brain, with studies reporting its ability to reduce neuroinflammation and alleviate neurodegenerative diseases, such as Parkinson's disease and Alzheimer's disease (AD).[22,23] Gal3 as a new ligand for TREM2 that promotes inflammatory response in AD.[24] Studies have shown that TREM2 attenuates LIRI and LPS-induced lung injury.[25,26] However, the roles and molecular mechanisms of TREM2 and Gal3 in LIRI remain to be studied. Therefore, we postulated that Gal3 might participate in the pathogenesis of LIRI by modulating macrophage polarization via TREM2 and substantiated this conjecture through both *in vivo* and *in vitro* experiments.

RESULTS

Inhibition of Gal3 alleviated lung tissues damage and inflammatory response induced by lung I/R in mice

To explore the function of Gal3 in mouse LIRI, we employed TD139 (a potent inhibitor of Gal3) to impede its activity. The outcomes obtained from western blots and ELISA assays demonstrated that TD139 significantly attenuated the expression level of Gal3 in LIRI (Figures 1A–1D). Morphological changes in lung tissue were evaluated via HE staining (Figure 1E). In the sham, DMSO, and TD139 groups, alveolar and pulmonary interstitial were clear and complete. The alveolar walls exhibited no signs of thickening or edema, while inflammatory infiltration was absent from the lung tissue. The lung tissue of I/R group exhibited severe hyperemia, destruction of alveolar structure, and extensive infiltration of inflammatory factors and erythrocytes. However, treatment with TD139 significantly attenuated these injuries. The lung injury score (Figure 1F) and lung tissue W/D ratio (Figure 1G) also corroborated these lung tissue alterations. We also observed changes in transmission electron microscopy at the ultrastructural level (Figure 1H). The sham, DMSO, and TD139 groups exhibited normal ultrastructure with intact basement membrane, clearly visible lamellar bodies (indicated by arrows), type II alveolar epithelial cell microvilli, and no mitochondrial swelling (triangles). In the I/R group, damage to the basement membrane, disappearance of the lamellar bodies and microvilli, and obvious swelling of mitochondria were observed. Whereas in the I/R + TD139 group, these changes were mitigated.

Additionally, we assessed the expression of inflammatory cytokines TNF-α, IL-1β, and IL-10 in BALF, serum, and lung tissue by ELISA (Figure 2). Compared to the sham, DMSO, and TD139 groups, there was a significant increase in pro-inflammatory cytokines TNF-α and IL-1β expression while anti-inflammatory cytokine IL-10 expression decreased in the I/R group. Inhibiting Gal3 effectively reversed the trend of inflammatory response induced by lung I/R. In summary, our findings demonstrate that inhibition of Gal3 can ameliorate lung tissues damage and inflammatory response induced by lung I/R in mice.

Inhibition of Gal3 reduced macrophage M1-type polarization and increased M2-type polarization in LIRI mice model

Given Gal3's ability to modulate inflammatory factors in LIRI, it is plausible that Gal3 may also play a role in regulating macrophage polarization. To this end, we assessed the expression of M1-type macrophage markers (IL-1β, IL-6, TNF-α, CCL5) and M2-type macrophage markers (Arg1, IL-10, Retnla, Chil3).[27] The western blot results demonstrated a significant increase in the protein expression of IL-1β, IL-6, TNF-α, and CCL5 after I/R. However, pretreatment with TD139 effectively attenuated these changes (Figures 3A–3E). In order to evaluate the trend of macrophage polarization more intuitively, we selected IL-1β and IL-6 for immunofluorescence staining (Figures 3F and 3G). The results showed that the expression of IL-1β and IL-6 was low in the sham, DMSO, and TD139 groups. Pretreatment with TD139 reduced the high expression of IL-1β and IL-6 induced by lung I/R in macrophages. Similarly, we detected the protein expression of M2-type markers (Figures 4A–4E). Notably, levels of Arg1, IL-10, Retnla and Chil3 were significantly elevated in the I/R group compared to those in the sham group. Arg1 and IL-10 were selected for immunofluorescence staining (Figures 4F and 4G). The results showed that the expression of Arg1 and IL-10 in macrophages was significantly increased in the I/R + TD139 group compared to the I/R group. These
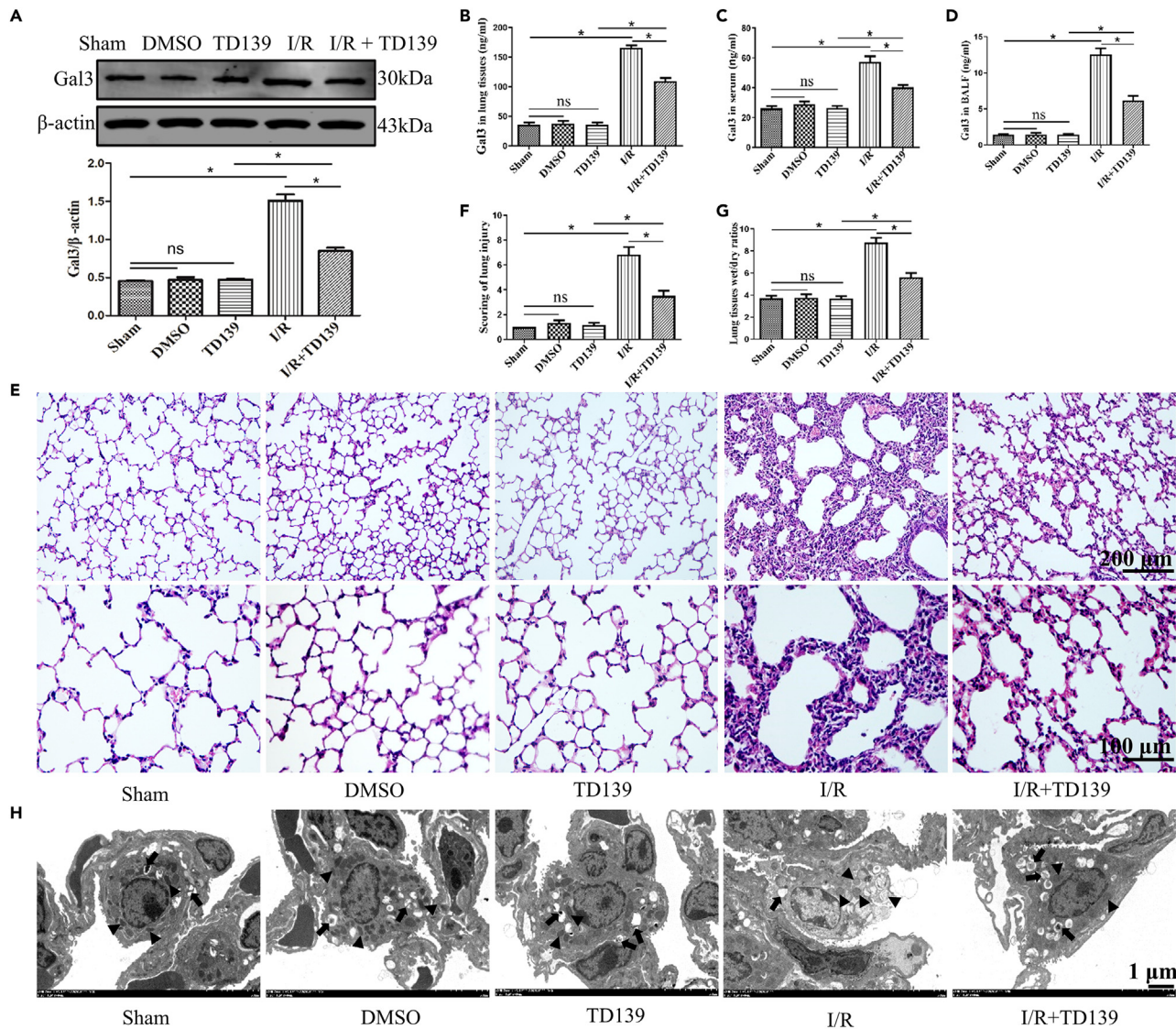
Figure 1. Gal3 inhibition reduced lung tissues damage induced by lung I/R

(A) The Gal3 protein expression in lung tissue was assessed by western blotting, and the density of Gal3 (relative to β-actin) on western blotting was quantified (n = 3).

(B–D) The expression of Gal3 in lung tissue, BALF and serum was detected by ELISA (n = 6).

(E) Paraffin-embedded lung tissue sections were stained with hematoxylin and eosin (n = 3) at magnifications of 200×, scale bar 200 μm and 400X, scale bar 100 μm.

(F) The extent of lung injury was assessed by scoring the F images (n = 6 section per group).

(G) The W/D ratio of lung tissue (n = 6).

(H) Ultrastructural changes were evaluated through transmission electron microscopy. Arrows indicate lamellar body and triangles mitochondria (n = 3). Scale bar, 1 μm. The data were mean ± SEM. One-way analysis of variance was used for data comparison, ns, not significant, *p < 0.05, was statistically significant.

findings suggest that Gal3 inhibition can reverse M1-type macrophage polarization while promoting M2-type macrophage differentiation in an LIRI mouse model.

Inhibition of Gal3 attenuated cell injury and regulated macrophage polarization *in vitro* OGD/R model

To further validate the regulatory role of Gal3 in macrophage polarization, we established an OGD/R RAW264.7 cell model.[28] Firstly, we assessed the protein expression of Gal3 by western blotting (Figures 5A and 5B). Compared to DMSO and TD139 groups, Gal3 expression was upregulated in the
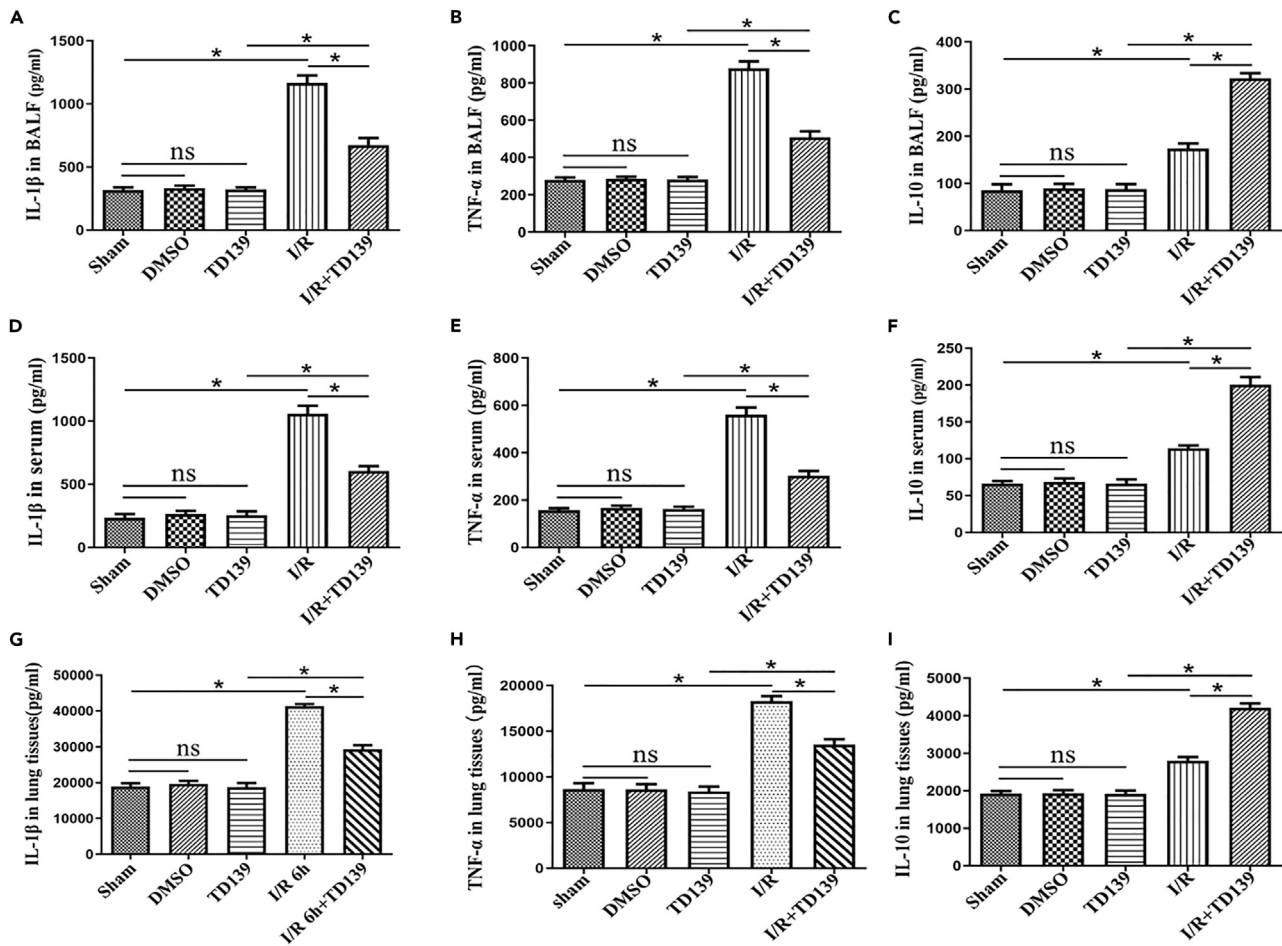
Figure 2. Gal3 inhibition attenuated the inflammatory response induced by lung I/R

(A–C) BALF of left lung after lung I/R was collected, and the supernatant was extracted to detect the contents of TNF-α, IL-1β, and IL-10 in BALF.

(D–F) After LIRI, the heart blood was taken, and the supernatant was collected by centrifugation after standing at low temperature for 3 h. The levels of TNF-α, IL-1β, and IL-10 in the serum were detected.

(G–I) The lung tissue was subjected to standard treatment to detect the contents of TNF-α, IL-1β, and IL-10 in lung tissue. Data shown are mean ± SEM from n = 6 per group, ns, no statistical significance, *p < 0.05, was statistically significant.

OGD/R + DMSO group. However, pretreatment with TD139 significantly attenuated the induction of Gal3 expression caused by OGD/R insult. Moreover, while cell viability decreased to 26% in the OGD/R + DMSO group, this change was reversed upon treatment with TD139 in the OGD/R + TD139 group.

Then, we quantified the protein expression levels of M1-type macrophage markers (IL-1β, IL-6, TNF-α, CCL5) and M2-type macrophage markers (Arg1, IL-10, Retnla, Chil3). The results were consistent with those obtained from animal experiments. Specifically, our findings demonstrated that OGD/R significantly upregulated the expression of M1-type macrophage markers, however, this effect was reversed by TD139 treatment (Figures 5D–5H). Furthermore, TD139 treatment resulted in a further increase in the slightly elevated expression of M2-type macrophage markers induced by OGD/R (Figures 6A–6E). Similarly, cyto-immuno-fluorescence staining was performed to confirm that Gal3 inhibition reduced macrophage polarization toward the M1 phenotype (Figures 5I and 5J) and increased polarization toward the M2 phenotype (Figures 6F and 6G) in an OGD/R vitro model.

Gal3 and TREM2 colocalized in macrophages and Gal3 inhibited the expression of TREM2 in LIRI

Gal3 has been reported as a new ligand in TREM2.[24] Prompting us to investigate the regulation of Gal3 on TREM2 in both *in vivo* and vitro models. Our initial findings revealed co-localization of Gal3 and TREM2
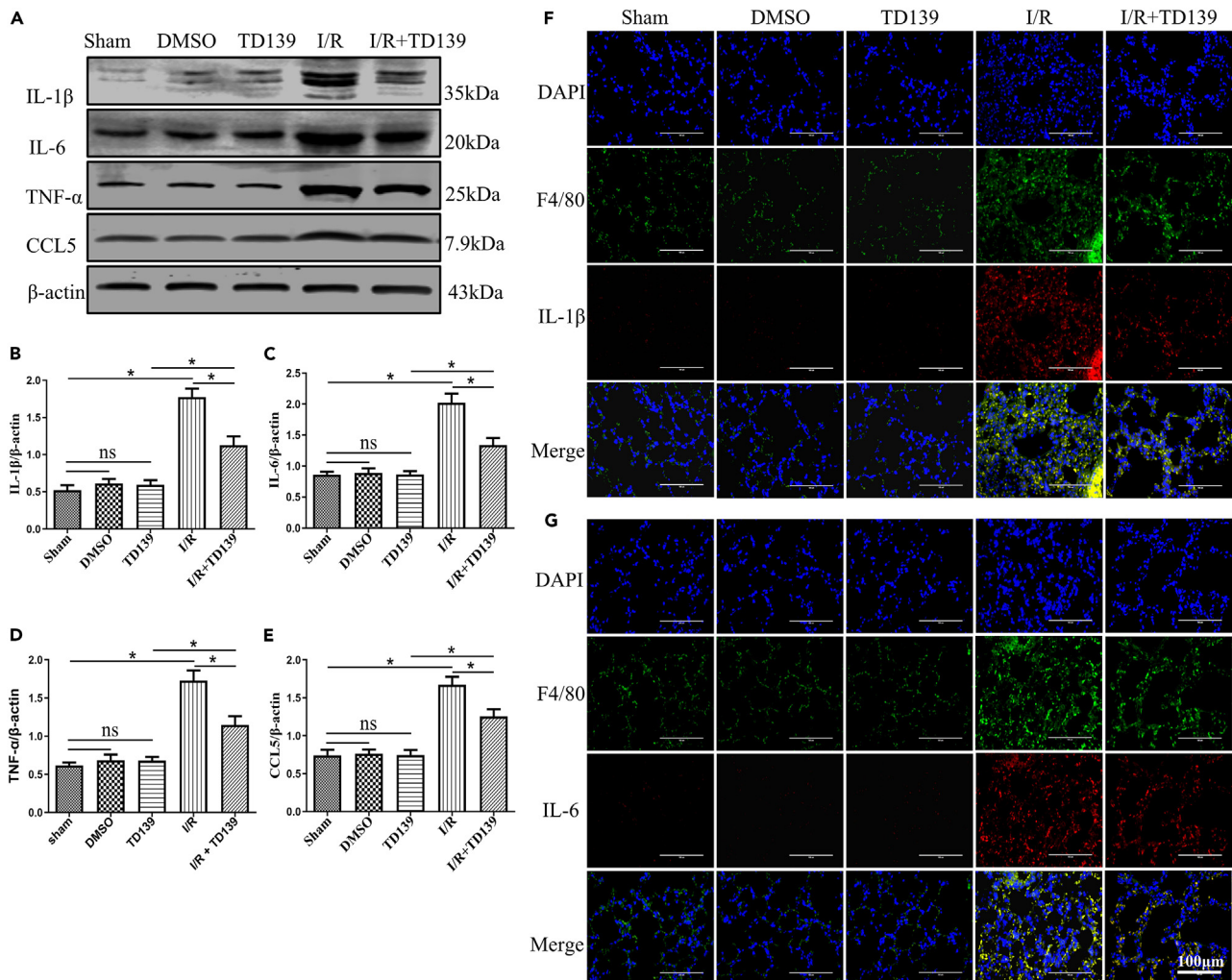
Figure 3. Inhibition of Gal3 reduces the expression of M1-type macrophages induced by lung I/R

(A) Western blot of IL-1β, IL-6, TNF-α, and CCL5 in lung tissues.

(B–E) Density analysis of IL-1β, IL-6, TNF-α, and CCL5 relative to β-actin in part A. (n = 3, mean $\pm$ SEM, ns, no statistical significance, *p < 0.05).

(F and G) Lung tissues were stained with macrophages marker (F4/80, green), anti-IL-1β (red), and anti-IL-6 antibodies (red). Nuclei were stained with DAPI (blue). Magnification, 400×, scale bar, 100 μm.

within macrophages present in lung tissue (Figures 7A and 7B). After lung I/R, macrophage and Gal3 expression increased significantly, while TREM2 expression decreased and the co-localization between Gal3 and TREM2 was reduced (white dotted line marking the figure). However, pretreatment with TD139 resulted in increased expression levels of TREM2 which had been previously suppressed due to lung I/R. We subsequently employed western blotting and RT-qPCR to quantify the protein and mRNA expression of TREM2 in vivo and vitro LIRI models (Figures 7C–7F), which yielded results consistent with those obtained from immunofluorescence. In conclusion, we determined that Gal3 co-localizes with TREM2 in macrophages and Gal3 inhibited the expression of TREM2 in LIRI.

TREM2 protected against LIRI by inducing M2-type macrophage polarization

To further substantiate the involvement of TREM2 in macrophage polarization during LIRI, we conducted validation experiments using TREM2 knockout mice (TREM2$^{-/-}$) and heat shock protein 60 (HSP60), a mitochondrial chaperone protein that is expressed on the surface of various cell types and functions as an agonist for TREM2.[29] We initially employed western blotting to detect TREM2 protein expression in lung tissues, aiming to verify the knockout efficiency of TREM2 and the impact of HSP60 on its expression in vivo.
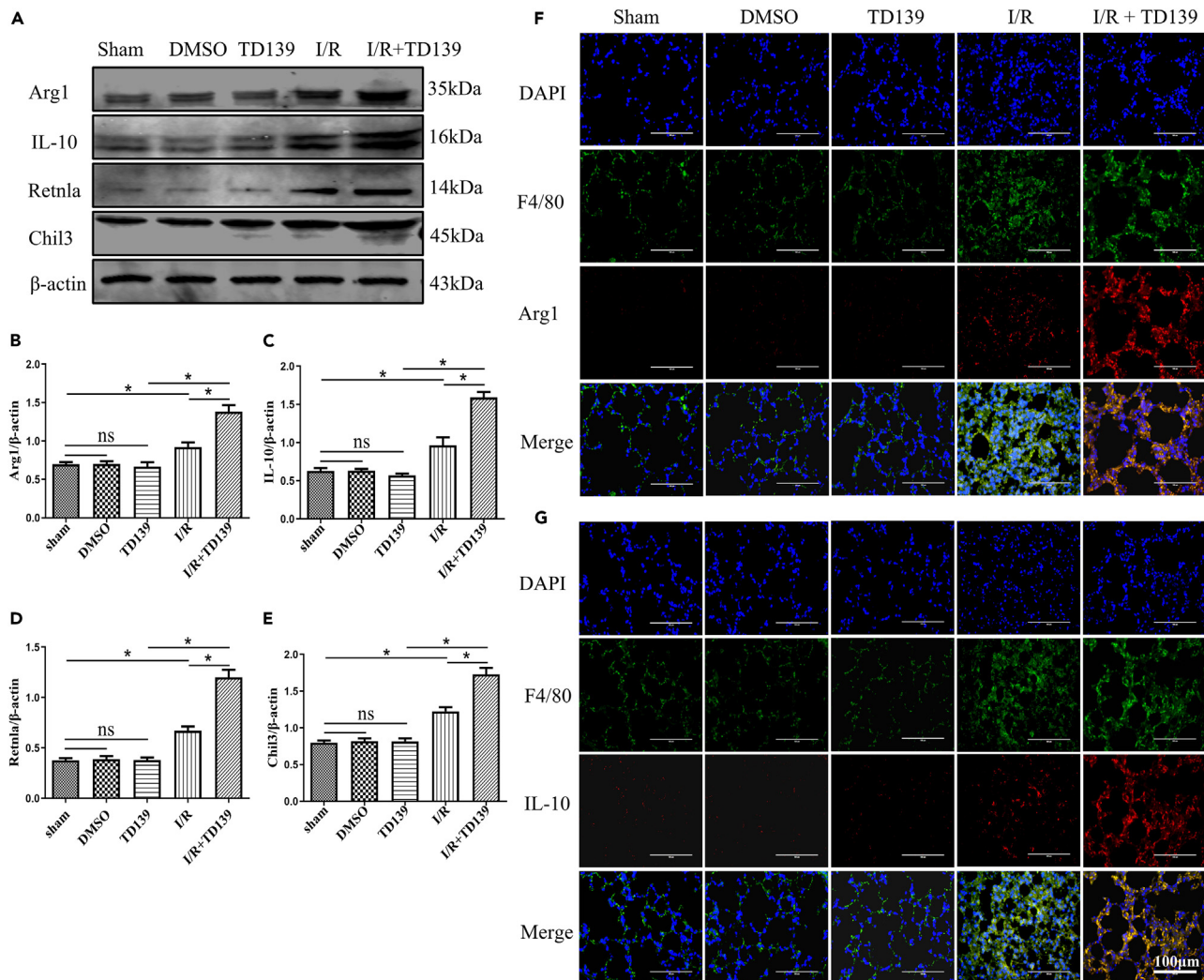
Figure 4. Inhibition of Gal3 increases the expression of M2 type macrophages induced by lung I/R

(A) Western blot of Arg1, IL-10, Retnla, and Chil3 in lung tissues.

(B–E) Density analysis of Arg1, IL-10, Retnla, and Chil3 relative to β-actin in part A. (n = 3, mean ± SEM, ns, no statistical significance, *p < 0.05).

(F and G) Lung tissues were stained with macrophages marker (F4/80, green), anti-Arg1 (red), and anti-IL-10 antibodies (red). Nuclei were stained with DAPI (blue). Magnification, 400×, scale bar, 100 μm.

The results from our western blot analysis (Figure 8A) demonstrated that there was negligible TREM2 expression in the TREM2$^{-/-}$ group, while HSP60 treatment led to an increase in TREM2 expression. Notably, inhibition of Gal3 and addition of HSP60 had a synergistic effect on promoting TREM2 expression. Subsequently, we assessed morphological changes in lung tissue with HE staining (Figure 8B). The findings indicated that the I/R + TREM2$^{-/-}$ group exhibited more severe lung tissue damage than the I/R group, characterized by almost no intact alveolar structures, severe tissue congestion and edema, and extensive infiltration of inflammatory cells. However, activation of TREM2 expression significantly ameliorated these pathological changes. Additionally, we observed that the most potent reversal of I/R-induced lung tissue injury occurred when activation of TREM2 expression was accompanied by inhibition of Gla3. The findings were further supported by the lung tissue injury score and W/D ratio (Figures 8C and 8D). We subsequently performed immunofluorescence staining to detect and analyze the expression of macrophage polarization markers IL-1β and Arg1 in lung tissues (Figures 8E–8H). As indicated by the results, the I/R + TREM2$^{-/-}$ group exhibited the most prominent and significant M1-type polarization fluorescence expression compared to other groups, while the polarization expression of M2-type macrophages was suppressed.
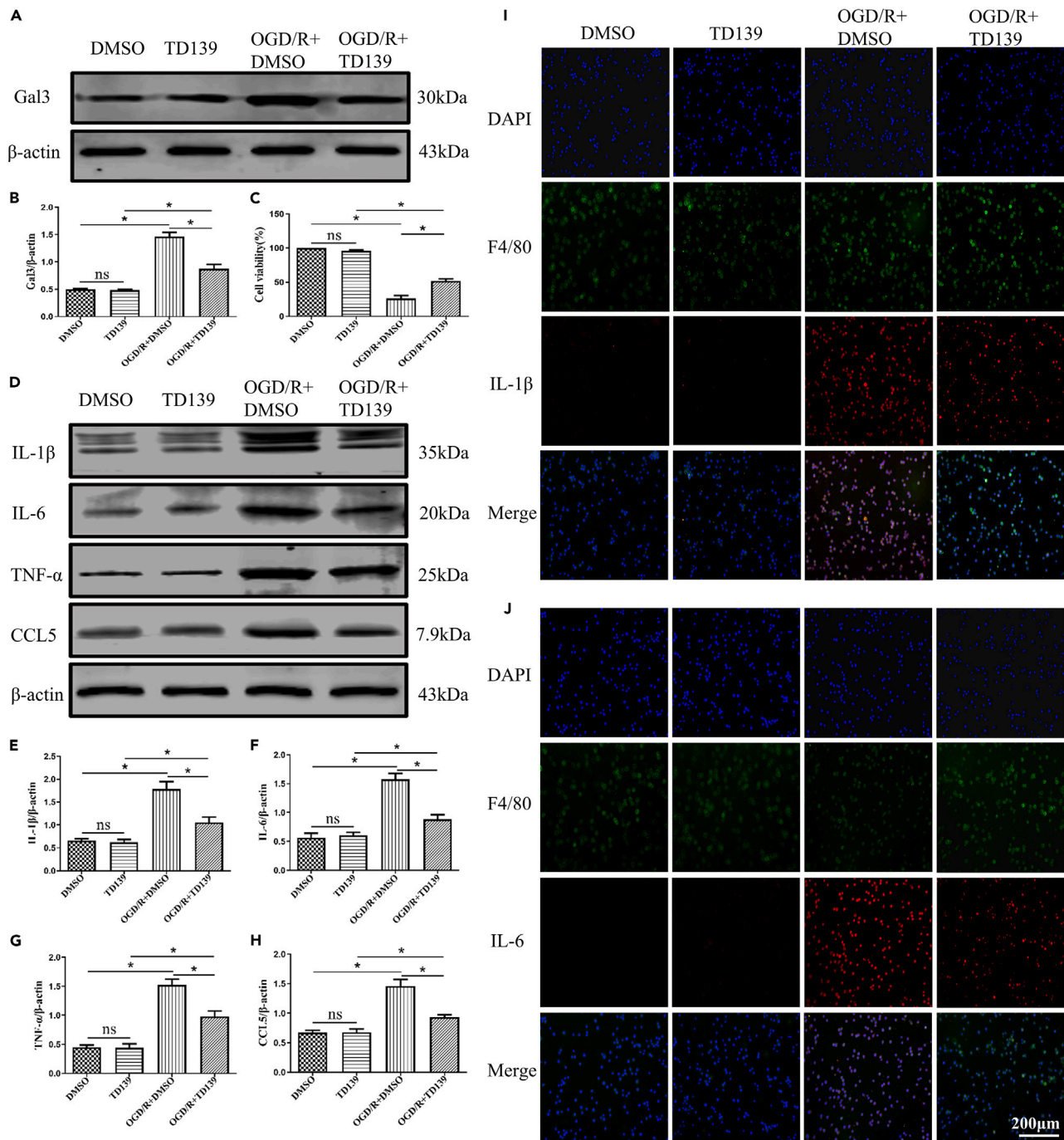
Figure 5. Gal3 inhibition reduces macrophage polarization toward M1-type in OGD/R vitro model

(A) Western blot of Gal3 in lung tissues.

(B) Density analysis of Gal3 relative to β-actin in part A.

(C) Cell viability was measured by CCK-8 assay (n = 6).

(D) Western blot of IL-1β, IL-6, TNF-α, and CCL5 in RAW264.7 cells.

(E–H) Densitometry of western blots in part D. Levels were standardized uniformly with β-actin. (n = 3, mean ± SEM, ns, no statistical significance, *p < 0.05).

(I and J) Immunofluorescence staining showed macrophages marker (F4/80, green), IL-1β (red), and IL-6 (red) in RAW264.7 cells. Nuclei were stained with DAPI (blue). Magnification, 200×, scale bar, 200 μm.
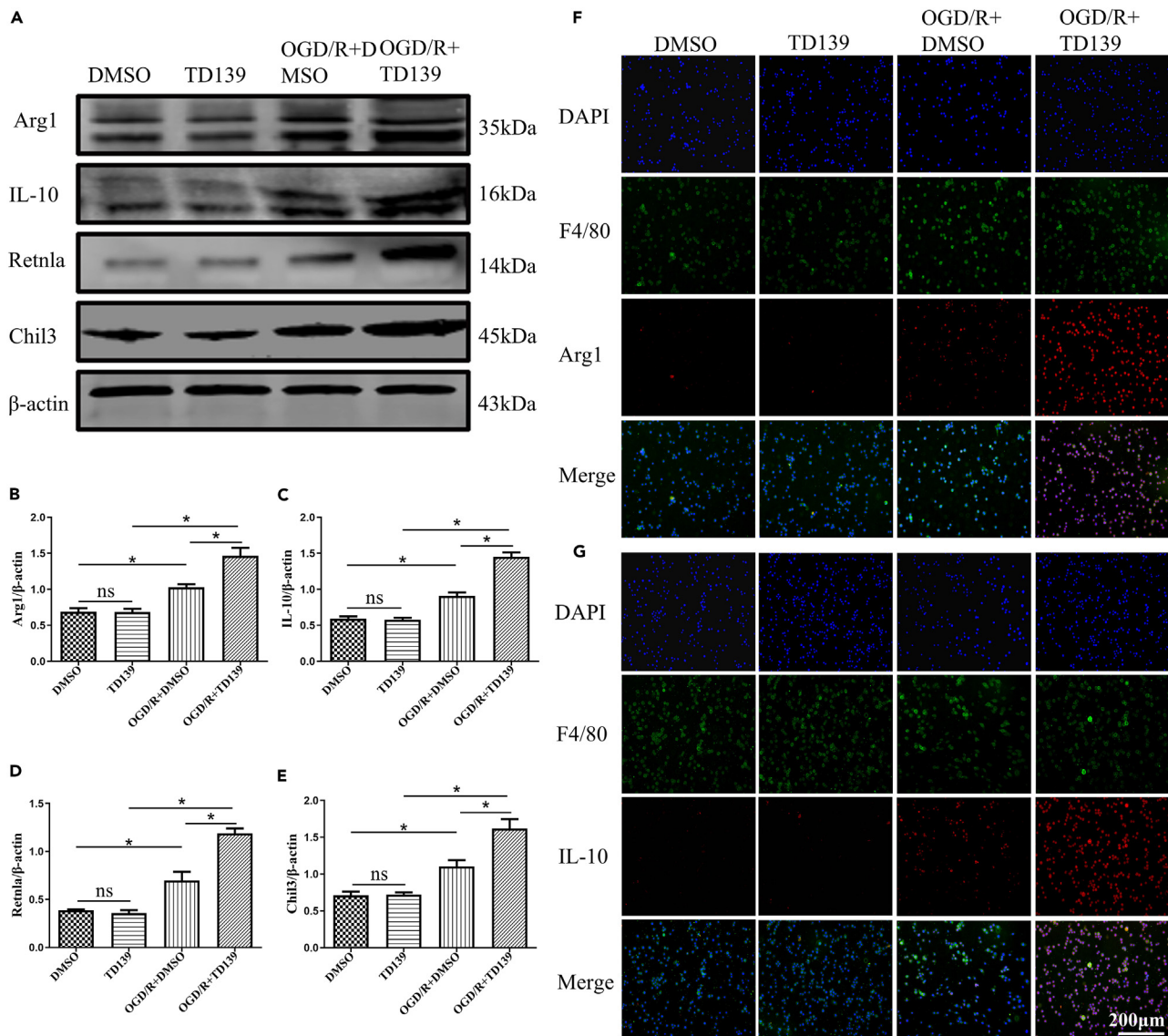
Figure 6. Gal3 inhibition promotes the polarization of macrophages toward the M2-type in OGD/R vitro model

(A) Western blot of Arg1, IL-10, Retnla, and Chil3 in RAW264.7 cells.

(B–E) Densitometry of western blots in part A. Levels were standardized uniformly with β-actin. (n = 3, mean ± SEM, ns, no statistical significance, *p < 0.05).

(F and G) Immunofluorescence staining showed macrophages marker (F4/80, green), Arg1 (red), and IL-10 (red) in RAW264.7 cells. Nuclei were stained with DAPI (blue). Magnification, 200×, scale bar, 200 μm.

Moreover, HSP60 was able to reverse these changes, whereas co-treatment with TD139 and HSP60 further enhanced M2-type macrophage polarization and attenuated M1-type macrophage polarization. The results confirm that TREM2 knockout exacerbates lung tissue injury by promoting M1-type macrophage polarization. Promoting TREM2 expression protects against LIRI by inducing M2-type macrophage polarization, while simultaneous inhibition of Gal3 has a more pronounced effect.

DISCUSSION

In this study, we assessed the potential therapeutic efficacy of Gal3 inhibition against LIRI *in vivo* and *in vitro* models. As demonstrated in our previous study, damage of lung tissue, alterations in lung ultrastructure and an increase in lung histopathological score were observed 2 h after lung I/R. The severity of the pulmonary damage was most pronounced at the 6-h mark. Subsequently, over a period of 12 h, there
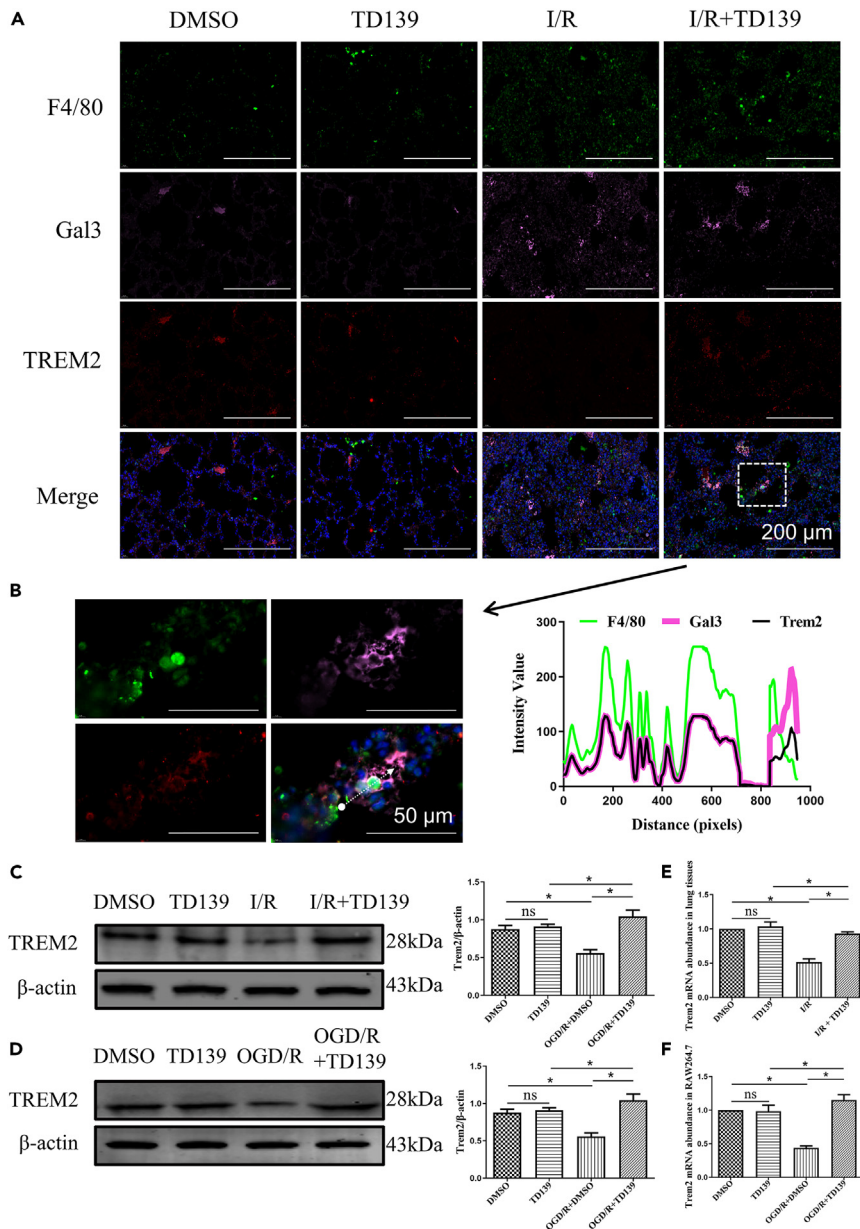
Figure 7. Gal3 and TREM2 colocalized in macrophages and Gal3 inhibited the expression of TREM2 in LIRI

(A) Macrophage markers (F4/80, green), anti-TREM2 antibody (red), and anti-Gal3 antibody (pink) were used for immunofluorescence co-localization staining of lung tissue. Magnification, 400×, scale bar, 200 μm.

(B) Enlarge the dotted box in part A. F4/80 (green), TREM2 (red), and Gal3 (pink) co-localization qualitative analysis. White dots to white triangles area (white dotted line) were analyzed with line intensity scans at higher magnification. Measurement of the intensity values demonstrated co-localization in those regions. Magnification, 2000×, scale bar, 50 μm.

(C) Western blotting and (E) RT-qPCR expression of TREM2 in lung tissue.

(D) Western blotting and (F) RT-qPCR expression of TREM2 in RAW264.7 cells. (n = 3, mean ± SEM, ns, no statistical significance, *p < 0.05).

was gradual amelioration of the lung injury and reduction in the corresponding histopathological score.[30] The survival rate of animal models within one day after surgery was 100% in all groups. Our findings indicate that mice subjected to LIRI exhibited severe inflammatory response and pathological changes in lung morphology and ultrastructure, and Gal3 inhibition effectively mitigated the effects induced

A

DMSO	+	+	+	+	+	+	+	+
TREM2⁻/⁻	−	+	−	−	−	+	−	+	−
HSP60	−	−	+	−	−	−	+	−	+
TD139	−	−	−	+	−	−	+	+
I/R	−	−	−	+	+	+	+	+	+

B

C   **D**   **G**   **H**

E

F
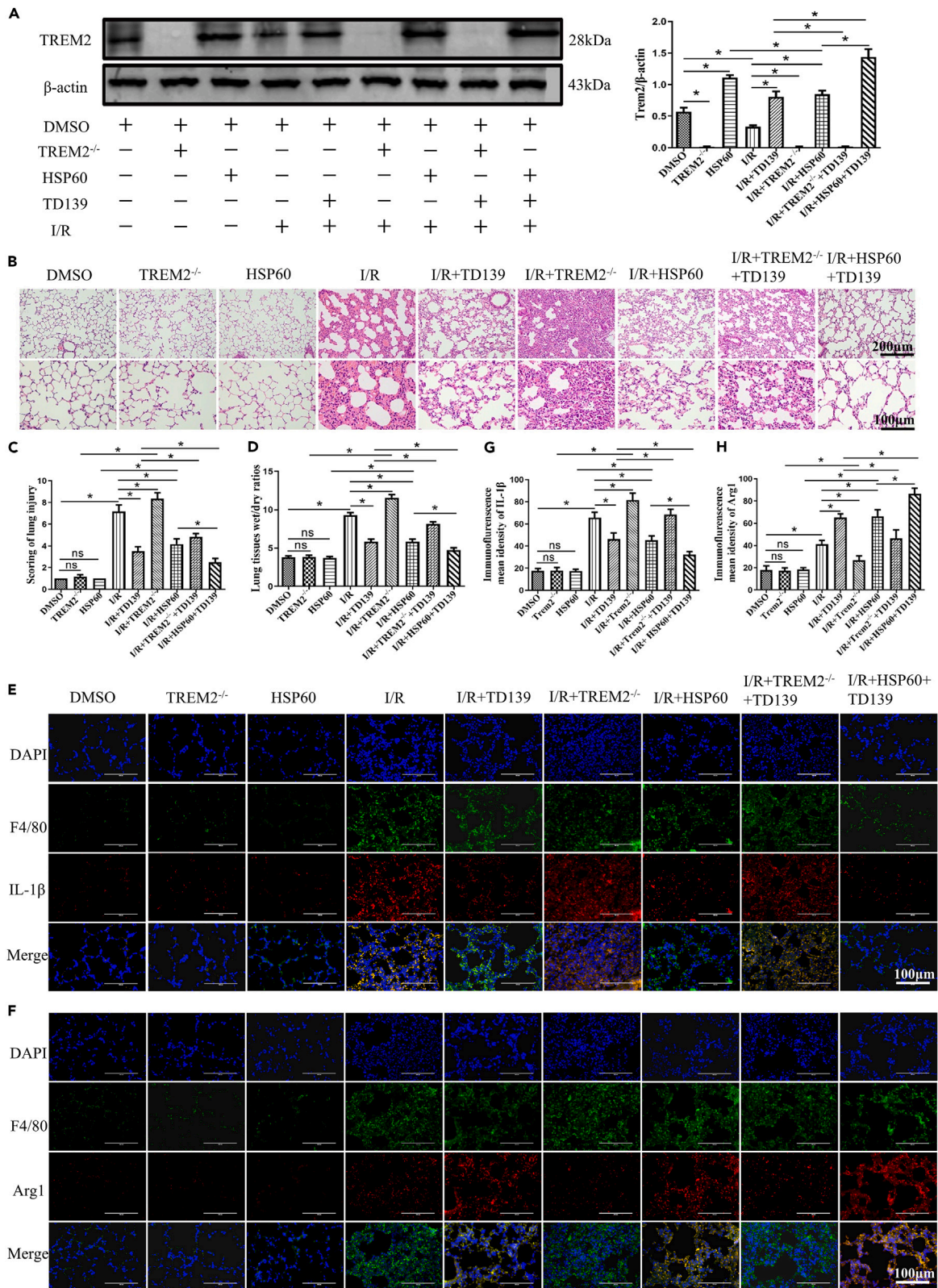
Figure 8. TREM2 protects LIRI

(A) Expression and quantitative analysis of TREM2 protein in lung tissue (n = 3).

(B) HE staining in lung tissue (n = 3), magnification, 200×, scale bar 200 μm and 400X, scale bar 100 μm.

(C) Scoring the extent of lung injury according to the image of B. (n = 6 section per group).

(D)The W/D ratio of lung tissue (n = 6).

(E and F) The left lung tissue sections were stained with macrophage marker (F4/80, green) with anti-IL-1β antibody (red) and anti-Arg1 antibody (red), respectively. Nuclei were stained with DAPI (blue) (n = 3). Magnification, 400×, scale bar, 100 μm.

(G and H) Immunofluorescence mean density of IL-1β and Arg1. ns, no statistical significance, *p < 0.05.

by lung I/R. These findings are in line with previous studies on the role of Gal3 in I/R injury,[31–33] indicating that targeting Gal3 inhibition may hold potential as a therapeutic strategy for LIRI-induced lung injury.

The immune response related to macrophages plays a crucial role in the pathogenesis of LIRI.[34] Although the extent of tissue damage during LIRI is dependent on the magnitude of the inflammatory response, which includes infiltrating macrophages and neutrophils, it has been observed that macrophages are the predominant type of cellular response. Currently, five activated macrophage phenotypes have been found, including M1 type macrophages, M2 type macrophages, CD169+ macrophages, TCR+ macrophages, and tumor-related macrophages (TAM).[35] M1 and M2 macrophage subtypes have been the most extensively investigated in scientific research, and these two phenotypes appear at different stages of inflammation.[36] Our study focuses on the role of macrophages in the inflammatory state of LIRI, specifically examining the transition between pro-inflammatory M1 phenotype and anti-inflammatory M2 phenotype. In the acute stage of ALI caused by various etiologies, M1-type macrophages are the predominant cells that release a plethora of inflammatory mediators (such as IL-1β, IL-6, TNF-α, etc.) to promote an inflammatory response and exacerbate tissue damage. Conversely, M2 macrophages facilitate lung tissue repair by producing anti-inflammatory cytokines (such as Arg1, IL-10, Retnla, Chil3) and promoting fibrosis in the later stages.[5,10,37] Our findings demonstrate that both Gal3 and macrophage polarization markers are upregulated *in vivo* and *in vitro* during I/R, with trends in Gal3 expression and M1-type polarization consistent with tissue injury and cell viability. Therefore, we propose that Gal3 may play a role in regulating macrophage polarization.

Gal3 can activate macrophages through various mechanisms, inducing inflammatory responses. Furthermore, activated macrophages are capable of producing Gal3, leading to a positive feedback amplification effect.[19,38] In acute brain inflammation, upregulated Gal3 binds to and stimulates microglia, leading to the pro-inflammatory M1-type polarization in the brain.[39] Meanwhile, deficiency of Gal3 can enhance the polarization of M2-type macrophages and alleviate concanavalin A (Con A)-induced liver injury.[40] We consistently observed close co-localization of Gal3 with macrophages in lung tissue. Inhibition of Gal3 expression resulted in a reduction of I/R-induced M1-type polarization levels and an upregulation of M2-type polarization levels both *in vivo* and *in vitro*, ultimately leading to the attenuation of pro-inflammatory factor release and alleviation of tissue and cell damage.

Boza-serrano et al. have demonstrated that Gal3 functions as an endogenous ligand of TREM2, which exerts a negative regulatory effect on brain inflammation in AD.[24] Our previous findings indicate that during LIRI, the expression of TREM2 is inversely correlated with lung injury and inflammatory response, the mechanism may be related to the effect of TREM2 on caspase-1 mediated pyroptosis.[30] The role of TREM2 in the inflammatory response caused by lung I/R is complex and varied. This study is a further in-depth study on the basis of previous studies. More importantly, this study confirms the regulatory role of Gal3 in TREM2 in LIRI.

TREM2 is predominantly expressed in DCs, macrophages and microglia, exerting its anti-inflammatory effects by inhibiting M1-type polarization while promoting M2-type polarization.[41] Our immunofluorescence staining results have demonstrated the co-localization of Gal3 and TREM2 in lung macrophages. Furthermore, inhibition of Gal3 has significantly upregulated TREM2 expression both *in vivo* and *in vitro*. Previous studies have shown that TREM2 plays a protective role against brain I/R[42] as well as liver I/R injury.[43] To elucidate the protective role of TREM2 in LIRI, we established LIRI models using both TREM2$^{-/-}$ and TREM2 agonists (HSP60). Our results demonstrated that, upon I/R insult, TREM2$^{-/-}$ mice exhibited more severe pulmonary edema and injury as well as a stronger M1-type polarization trend compared to wild-type mice. However, treatment with HSP60 reversed these changes and promoted

M2-type polarization. Meanwhile, we observed a significant upregulation of TREM2 upon concurrent inhibition of Gal3 and activation of TREM2 during LIRI, which was accompanied by more pronounced expression of M2 polarization markers and alleviated lung tissue damage. Therefore, our findings suggest that Gal3 inhibition can enhance TREM2 expression to cf. protection against LIRI. However, the regulatory mechanism of GAL3 on TREM2 is quite limited, further investigation is warranted to elucidate the specific molecular mechanism underlying the regulation of TREM2 by Gal3.

In summary, our studies of *in vivo* and *in vitro* injury models suggest that Gal3 inhibition can attenuate M1-type macrophage polarization and promote M2-type polarization to alleviate LIRI and I/R-induced inflammatory responses. This effect may be mediated by the upregulation of TREM2 expression. Our findings support the use of Gal3 antagonism as a new clinical target for treating LIRI.

Limitations of the study

The limitation of our study lies in the fact that while we have identified the co-localization of Gal3 and TREM2 in macrophages, as well as the regulation of TREM2 expression by Gal3, the specific molecular mechanism underlying Gal3's involvement in this regulatory process remains unexplored. And this will be the direction of our future research.

QUANTIFICATION AND STATISTICAL ANALYSIS

All data analyses were conducted using SPSS 25.0 software, with mean $\pm$ SEM used to express the data. One-way ANOVA was employed for comparisons between multiple groups, and Tukey's test was utilized for inter-group comparisons; differences of $p < 0.05$ were deemed statistically significant and represented by *. Graphpad Prism 8.0 was utilized to generate statistical plots.

STAR★METHODS

Detailed methods are provided in the online version of this paper and include the following:

- KEY RESOURCES TABLE
- RESOURCE AVAILABILITY
  - Lead contact
  - Materials availability
  - Data and code availability
- EXPERIMENTAL MODEL AND STUDY PARTICIPANT DETAILS
  - Animals
  - Lung ischemia reperfusion injury model
  - Cell culture and oxygen-glucose deprivation and reoxygenation (OGD/R) model
- METHOD DETAILS
  - Lung wet-to-dry ratio
  - Histopathological analysis
  - Transmission electron microscopy
  - Bronchoalveolar lavage fluid (BALF) acquisition and analysis
  - Enzyme-linked immunosorbent assay (ELISA)
  - Cell viability assays
  - Immunofluorescence staining
  - Western blotting
  - Total RNA extraction and real-time PCR

AUTHOR CONTRIBUTIONS

DECLARATION OF INTERESTS

REFERENCES

1. Fei, L., Jingyuan, X., Fangte, L., Huijun, D., Liu, Y., Ren, J., Jinyuan, L., and Linghui, P. (2020). Preconditioning with rHMGB1 ameliorates lung ischemia-reperfusion injury by inhibiting alveolar macrophage pyroptosis via the Keap1/Nrf2/HO-1 signaling pathway. J. Transl. Med. *18*, 301.

2. Gong, J., Ju, Y.N., Wang, X.T., Zhu, J.L., Jin, Z.H., and Gao, W. (2019). Ac2-26 ameliorates lung ischemia-reperfusion injury via the eNOS pathway. Biomed. Pharmacother. *117*, 109194.

3. Laubach, V.E., and Sharma, A.K. (2016). Mechanisms of lung ischemia-reperfusion injury. Curr. Opin. Organ Transplant. *21*, 246–252.

4. Johnston, L.K., Rims, C.R., Gill, S.E., McGuire, J.K., and Manicone, A.M. (2012). Pulmonary macrophage subpopulations in the induction and resolution of acute lung injury. Am. J. Respir. Cell Mol. Biol. *47*, 417–426.

5. Huang, X., Xiu, H., Zhang, S., and Zhang, G. (2018). The Role of Macrophages in the Pathogenesis of ALI/ARDS. Mediators Inflamm. *2018*, 1264913.

6. Martinez, F.O., and Gordon, S. (2014). The M1 and M2 paradigm of macrophage activation: time for reassessment. F1000Prime Rep. *6*, 13.

7. Shapouri-Moghaddam, A., Mohammadian, S., Vazini, H., Taghadosi, M., Esmaeili, S.A., Mardani, F., Seifi, B., Mohammadi, A., Afshari, J.T., and Sahebkar, A. (2018). Macrophage plasticity, polarization, and function in health and disease. J. Cell. Physiol. *233*, 6425–6440.

8. Rőszer, T. (2015). Understanding the Mysterious M2 Macrophage through Activation Markers and Effector Mechanisms. Mediators Inflamm. *2015*, 816460.

9. Sica, A., and Mantovani, A. (2012). Macrophage plasticity and polarization: in vivo veritas. J. Clin. Invest. *122*, 787–795.

10. Chen, X., Tang, J., Shuai, W., Meng, J., Feng, J., and Han, Z. (2020). Macrophage polarization and its role in the pathogenesis of acute lung injury/acute respiratory distress syndrome. Inflamm. Res. *69*, 883–895.

11. Saccon, F., Gatto, M., Ghirardello, A., Iaccarino, L., Punzi, L., and Doria, A. (2017). Role of galectin-3 in autoimmune and non-autoimmune nephropathies. Autoimmun. Rev. *16*, 34–47.

12. Sciacchitano, S., Lavra, L., Morgante, A., Ulivieri, A., Magi, F., De Francesco, G.P., Bellotti, C., Salehi, L.B., and Ricci, A. (2018). Galectin-3: One Molecule for an Alphabet of Diseases, from A to Z. Int. J. Mol. Sci. *19*, 379.

13. Haudek, K.C., Spronk, K.J., Voss, P.G., Patterson, R.J., Wang, J.L., and Arnoys, E.J. (2010). Dynamics of galectin-3 in the nucleus and cytoplasm. Biochim. Biophys. Acta *1800*, 181–189.

14. Davidson, P.J., Davis, M.J., Patterson, R.J., Ripoche, M.A., Poirier, F., and Wang, J.L. (2002). Shuttling of galectin-3 between the nucleus and cytoplasm. Glycobiology *12*, 329–337.

15. de Oliveira, F.L., Gatto, M., Bassi, N., Luisetto, R., Ghirardello, A., Punzi, L., and Doria, A. (2015). Galectin-3 in autoimmunity and autoimmune diseases. Exp. Biol. Med. *240*, 1019–1028.

16. Fulton, D.J.R., Li, X., Bordan, Z., Wang, Y., Mahboubi, K., Rudic, R.D., Haigh, S., Chen, F., and Barman, S.A. (2019). Galectin-3: A Harbinger of Reactive Oxygen Species, Fibrosis, and Inflammation in Pulmonary Arterial Hypertension. Antioxid. Redox Signal. *31*, 1053–1069.

17. Martínez-Martínez, E., Brugnolaro, C., Ibarrola, J., Ravassa, S., Buonafine, M., López, B., Fernández-Celis, A., Querejeta, R., Santamaria, E., Fernández-Irigoyen, J., et al. (2019). CT-1 (Cardiotrophin-1)-Gal-3 (Galectin-3) Axis in Cardiac Fibrosis and Inflammation. Hypertension *73*, 602–611.

18. Varasteh, Z., De Rose, F., Mohanta, S., Li, Y., Zhang, X., Miritsch, B., Scafetta, G., Yin, C., Sager, H.B., Glasl, S., et al. (2021). Imaging atherosclerotic plaques by targeting Galectin-3 and activated macrophages using ((89)Zr)-DFO- Galectin3-F(ab')(2) mAb. Theranostics *11*, 1864–1876.

19. Siew, J.J., Chen, H.-M., Chen, H.-Y., Chen, H.-L., Chen, C.-M., Soong, B.-W., Wu, Y.-R., Chang, C.-P., Chan, Y.-C., Lin, C.-H., et al. (2019). Galectin-3 is required for the microglia-mediated brain inflammation in a model of Huntington's disease. Nat. Commun. *10*, 3473.

20. Humphries, D.C., Mills, R., Dobie, R., Henderson, N.C., Sethi, T., and Mackinnon, A.C. (2021). Selective Myeloid Depletion of Galectin-3 Offers Protection Against Acute and Chronic Lung Injury. Front. Pharmacol. *12*, 715986.

21. Kober, D.L., and Brett, T.J. (2017). TREM2-Ligand Interactions in Health and Disease. J. Mol. Biol. *429*, 1607–1629.

22. Chen, S., Peng, J., Sherchan, P., Ma, Y., Xiang, S., Yan, F., Zhao, H., Jiang, Y., Wang, N., Zhang, J.H., and Zhang, H. (2020). TREM2 activation attenuates neuroinflammation and neuronal apoptosis via PI3K/Akt pathway after intracerebral hemorrhage in mice. J. Neuroinflammation *17*, 168.

23. Zhai, Q., Li, F., Chen, X., Jia, J., Sun, S., Zhou, D., Ma, L., Jiang, T., Bai, F., Xiong, L., and Wang, Q. (2017). Triggering Receptor Expressed on Myeloid Cells 2, a Novel Regulator of Immunocyte Phenotypes, Confers Neuroprotection by Relieving Neuroinflammation. Anesthesiology *127*, 98–110.

24. Boza-Serrano, A., Ruiz, R., Sanchez-Varo, R., García-Revilla, J., Yang, Y., Jimenez-Ferrer, I., Paulus, A., Wennström, M., Vilalta, A., Allendorf, D., et al. (2019). Galectin-3, a novel endogenous TREM2 ligand, detrimentally regulates inflammatory response in Alzheimer's disease. Acta Neuropathol. *138*, 251–273.

25. Fangte, L., Hao, L., Xiaojing, H., Chunxia, L., Siyi, W., Yi, Q., Linghui, P., and Fei, L. (2021). HSP60 attenuates lung ischemia-reperfusion injury by upregulating TREM2 expression. J. Guangxi Med. Univ. *38*, 877–881. Chinese.

26. Su, V.Y.F., Yang, K.Y., Chiou, S.H., Chen, N.J., Mo, M.H., Lin, C.S., and Wang, C.T. (2019). Induced Pluripotent Stem Cells Regulate Triggering Receptor Expressed on Myeloid Cell-1 Expression and the p38 Mitogen-Activated Protein Kinase Pathway in Endotoxin-Induced Acute Lung Injury. Stem Cell. 37, 631–639.

27. Li, Z., Martin, M., Zhang, J., Huang, H.Y., Bai, L., Zhang, J., Kang, J., He, M., Li, J., Maurya, M.R., et al. (2017). Kruppel-Like Factor 4 Regulation of Cholesterol-25-Hydroxylase and Liver X Receptor Mitigates Atherosclerosis Susceptibility. Circulation 136, 1315–1330.

28. Ryou, M.G., and Mallet, R.T. (2018). An In Vitro Oxygen-Glucose Deprivation Model for Studying Ischemia-Reperfusion Injury of Neuronal Cells. Methods Mol. Biol. 1717, 229–235.

29. Stefano, L., Racchetti, G., Bianco, F., Passini, N., Gupta, R.S., Panina Bordignon, P., and Meldolesi, J. (2009). The surface-exposed chaperone, Hsp60, is an agonist of the microglial TREM2 receptor. J. Neurochem. 110, 284–294.

30. Liang, F., Liu, H., He, X., Liu, C., Wu, S., Qin, Y., Pan, L., and Lin, F. (2021). Role and regulatory mechanism of triggering receptor expressed on myeloid cells 2 in mice lung ischemia/reperfusion injury. Zhonghua Wei Zhong Bing Ji Jiu Yi Xue 33, 933–937. Chinese.

31. Fernandes Bertocchi, A.P., Campanhole, G., Wang, P.H.M., Gonçalves, G.M., Damião, M.J., Cenedeze, M.A., Beraldo, F.C., de Paula Antunes Teixeira, V., Dos Reis, M.A., Mazzali, M., et al. (2008). A Role for galectin-3 in renal tissue damage triggered by ischemia and reperfusion injury. Transpl. Int. 21, 999–1007.

32. Ibarrola, J., Matilla, L., Martínez-Martínez, E., Gueret, A., Fernández-Celis, A., Henry, J.P., Nicol, L., Jaisser, F., Mulder, P., Ouvrard-Pascaud, A., and López-Andrés, N. (2019). Myocardial Injury After Ischemia/Reperfusion Is Attenuated By Pharmacological Galectin-3 Inhibition. Sci. Rep. 9, 9607.

33. Prud'homme, M., Coutrot, M., Michel, T., Boutin, L., Genest, M., Poirier, F., Launay, J.M., Kane, B., Kinugasa, S., Prakoura, N., et al. (2019). Acute Kidney Injury Induces Remote Cardiac Damage and Dysfunction Through the Galectin-3 Pathway. JACC. Basic Transl. Sci. 4, 717–732.

34. Naidu, B.V., Krishnadasan, B., Farivar, A.S., Woolley, S.M., Thomas, R., Van Rooijen, N., Verrier, E.D., and Mulligan, M.S. (2003). Early activation of the alveolar macrophage is critical to the development of lung ischemia-reperfusion injury. J. Thorac. Cardiovasc. Surg. 126, 200–207.

35. Chávez-Galán, L., Olleros, M.L., Vesin, D., and Garcia, I. (2015). Much More than M1 and M2 Macrophages, There are also CD169+ and TCR+ Macrophages. Front. Immunol. 6, 263.

36. Zhang, M., Nakamura, K., Kageyama, S., Lawal, A.O., Gong, K.W., Bhetraratana, M., Fujii, T., Sulaiman, D., Hirao, H., Bolisetty, S., et al. (2018). Myeloid HO-1 modulates macrophage polarization and protects against ischemia-reperfusion injury. JCI Insight 3, e120596.

37. Patel, U., Rajasingh, S., Samanta, S., Cao, T., Dawn, B., and Rajasingh, J. (2017). Macrophage polarization in response to epigenetic modifiers during infection and inflammation. Drug Discov. Today 22, 186–193.

38. Sunil, V.R., Francis, M., Vayas, K.N., Cervelli, J.A., Choi, H., Laskin, J.D., and Laskin, D.L. (2015). Regulation of ozone-induced lung inflammation and injury by the beta-galactoside-binding lectin galectin-3. Toxicol. Appl. Pharmacol. 284, 236–245.

39. Burguillos, M.A., Svensson, M., Schulte, T., Boza-Serrano, A., Garcia-Quintanilla, A., Kavanagh, E., Santiago, M., Viceconte, N., Oliva-Martin, M.J., Osman, A.M., et al. (2015). Microglia-Secreted Galectin-3 Acts as a Toll-like Receptor 4 Ligand and Contributes to Microglial Activation. Cell Rep. 10, 1626–1638.

40. Volarevic, V., Milovanovic, M., Ljujic, B., Pejnovic, N., Arsenijevic, N., Nilsson, U., Leffler, H., and Lukic, M.L. (2012). Galectin-3 deficiency prevents concanavalin A-induced hepatitis in mice. Hepatology 55, 1954–1964.

41. Zhang, J., Zheng, Y., Luo, Y., Du, Y., Zhang, X., and Fu, J. (2019). Curcumin inhibits LPS-induced neuroinflammation by promoting microglial M2 polarization via TREM2/TLR4/NF-kappaB pathways in BV2 cells. Mol. Immunol. 116, 29–37.

42. Wu, R., Li, X., Xu, P., Huang, L., Cheng, J., Huang, X., Jiang, J., Wu, L.J., and Tang, Y. (2017). TREM2 protects against cerebral ischemia/reperfusion injury. Mol. Brain 10, 20.

43. Nakao, T., Ono, Y., Dai, H., Nakano, R., Perez-Gutierrez, A., Camirand, G., Huang, H., Geller, D.A., and Thomson, A.W. (2019). DNAX Activating Protein of 12 kDa/Triggering Receptor Expressed on Myeloid Cells 2 Expression by Mouse and Human Liver Dendritic Cells: Functional Implications and Regulation of Liver Ischemia-Reperfusion Injury. Hepatology 70, 696–710.

44. Volarevic, V., Markovic, B.S., Bojic, S., Stojanovic, M., Nilsson, U., Leffler, H., Besra, G.S., Arsenijevic, N., Paunovic, V., Trajkovic, V., and Lukic, M.L. (2015). Gal-3 regulates the capacity of dendritic cells to promote NKT-cell-induced liver injury. Eur. J. Immunol. 45, 531–543.

45. Li, H., Xiao, L., He, H., Zeng, H., Liu, J., Jiang, C., Mei, G., Yu, J., Chen, H., Yao, P., and Tang, Y. (2021). Quercetin Attenuates Atherosclerotic Inflammation by Inhibiting Galectin-3-NLRP3 Signaling Pathway. Mol. Nutr. Food Res. 65, e2000746.

46. Wang, T., Liu, C., Pan, L.H., Liu, Z., Li, C.L., Lin, J.Y., He, Y., Xiao, J.Y., Wu, S., Qin, Y., et al. (2020). Inhibition of p38 MAPK Mitigates Lung Ischemia Reperfusion Injury by Reducing Blood-Air Barrier Hyperpermeability. Front. Pharmacol. 11, 569251.

STAR★METHODS

KEY RESOURCES TABLE

REAGENT or RESOURCE	SOURCE	IDENTIFIER
Antibodies		
anti-Galectin 3, mouse monoclonal	Abcam	Cat #ab2785; RRID: AB_303298
anti-TREM2, rabbit polyclonal	bioss	Cat #bs2723R; RRID: AB_10856501
anti-F4/80 rat monoclonal	Abcam	Cat #ab6640; RRID: AB_1140040
anti-IL-1β, goat polyclonal	R&D systems	Cat #AF-401-NA; RRID: AB_416684
anti-TNF-α, rabbit monoclonal	Abcam	Cat #ab183218; RRID: AB_2889388
anti-IL-6, rabbit polyclonal	Novus Biologicals	Cat #NB600-1131; RRID: AB_10001997
anti-CCL5, goat polyclonal	R&D systems	Cat #AF478; RRID: AB_355385
anti- Arginase 1, rabbit polyclonal	Novus Biologicals	Cat #NBP1-32731; RRID: AB_10003985
goat polyclonal	R&D systems	Cat #AF519; RRID: AB_355408
rabbit polyclonal	Abcam	Cat #ab39626; RRID: AB_777652
anti-Chitinase 3-like 3,rat monoclonal	R&D systems	Cat #MAB2446; RRID: AB_2079007
goat anti-mouse H&L IRDye@800 CW	Abcam	Cat #ab216772; RRID: AB_2857338
goat anti-rabbit H&L IRDye@800 CW	Abcam	Cat #ab216773; RRID: AB_2925189
donkey anti-goat H&L IRDye@800 CW	Abcam	Cat #ab216775; RRID: AB_2893338
Alexa donkey anti-rat 488	Abcam	Cat #ab150153; RRID: AB_2737355
Alexa donkey anti- rabbit 594	Abcam	Cat #ab150076; RRID: AB_2782993
Alexa donkey anti- goat 594	Abcam	Cat #ab150132; RRID: AB_2810222
Chemicals, peptides, and recombinant proteins		
TD139	GLPBIO	Cat #GC19350
DMSO	Solarbio	Cat #D8371
Dulbecco's modified Eagle's medium (DMEM)	Gibco	Cat #C11995500BT
fetal bovine serum (FBS)	Gibco	Cat #10099-141
phosphate-buffered saline (PBS)	Servicebio	Cat #G4202
RIPA buffer	Solarbio	Cat #R0010
protease inhibitor cocktail	Servicebio	Cat #G2006
phosphatase inhibitor cocktail	Cell Signaling Technology	Cat #CST_5872s

Continued

REAGENT or RESOURCE	SOURCE	IDENTIFIER
Critical commercial assays		
IL-1β ELISA kit	CUSABIO	Cat #CSB-E08054m
TNF-α ELISA kit	CUSABIO	Cat #CSB-E04741m
IL-10 ELISA kit	CUSABIO	Cat #CSB-E04594m
Gal3 ELISA kit	CUSABIO	Cat #CSB-E14296m
CCK-8 kit	Beyotime Biotechnology	Cat #C0038
Bicinchoninic acid kit	Beyotime Biotechnology	Cat #P0011
RNAiso plus	Takara	Cat #9109
Prime Script™ RT kit	Takara	Cat #RR047A
Experimental models: Organisms/strains		
Mouse: C57BL/6	Animal Center of Guangxi Medical University	N/A
Mouse: C57BL/6N-TREM2em1cyagen	Cyagen Biotechnology	N/A
Mouse mononuclear macrophage leukemia cells (RAW264.7 cells)	Procell Life Science & Technology Co, Ltd	Cat#CL-0190
Oligonucleotides		
qPCR primers: GAPDH Forward: 5′-AGGTCGGTGTGAACGGATTTG-3′ Reverse: 5′-TGTAGACCATGTAGTTGAGGTCA-3′	This paper	N/A
qPCR primers: TREM2 Forward: 5′-CTGGAACCGTCACCATCACTC-3′ Reverse: 5′-CGAAACTCGATGACTCCTCGG-3′	This paper	N/A
Genotyping primers: C57BL/6N-TREM2em1cyagen mice Forward: F1: 5′-GATGTCTTAAATAGAGCCAGAGGG-3′, F2: 5′-AGTACATTCAGGGATTCCACAGGTC-3′ Reverse: 5′-GGAAGGTGGTAGGCTAGAGGTGAC-3′	This paper	N/A

RESOURCE AVAILABILITY

Lead contact

Further information and requests for resources and reagents should be directed to and will be fulfilled by the lead contact, Fei Lin (linfei@gxmu.edu.cn).

Materials availability

This study did not generate new unique reagents.

Data and code availability

This study did not generate new datasets.

This study did not generate new code.

Any additional information will be available from the lead contact upon request.

EXPERIMENTAL MODEL AND STUDY PARTICIPANT DETAILS

Animals

Adult male C57BL/6 and C57BL/6N-TREM2^{em1cyagen} (TREM2$^{-/-}$) mice aged 6–8 weeks and weighing 20-25g, were purchased from the Animal Centre of Guangxi Medical University and Cyagen Biotechnology (Suzhou, China). Animals were kept in specific pathogen-free conditions with 12 hours of light / 12 hours of darkness per day, and maintained with conventional feed. Amplification of TREM2 gene sequences from genomic DNA of tail-clipped mice to determine the genotype of the offspring. All animal experiments were approved by the Institutional Animal Care and Use Committee of Guangxi Medical University (Nanning, China).

Lung ischemia reperfusion injury model

Mice were randomly divided into to five groups (n = 9 per group): sham, DMSO, TD139 (a new synthetic Gal3 inhibitor with high affinity for Gal3, dissolved in DMSO), I/R (ischemia reperfusion), and I/R + TD139. The mice were anesthetized via intraperitoneal injection of sodium pentobarbital at a dosage of 50 mg/kg. After successful insertion of a 20G plastic catheter via oral endotracheal intubation, the mice were connected to an animal ventilator set at a tidal volume of 10 ml/kg and respiratory rate of 100–130 breaths/min for mechanical ventilation. Intraperitoneal injection of 1% DMSO or TD139 (15 mg/kg) was administered 2 hours prior to thoracotomy and repeated 2 hours after ischemia induction.[40,44] The sham, DMSO, and TD139 groups underwent thoracotomy without clamping the pulmonary hilum. In the I/R and I/R + TD139 groups, left thoracotomy was performed in the third intercostal space to expose the left pulmonary hilum which was then clamped for 1 hour. During single-lung ventilation, the tidal volume was reduced to 6 ml/kg and the respiratory rate was increased to 150 breaths/min. The surgical incision was covered with gauze soaked in sterile saline solution. After the ischemia, the clamp was removed and subsequently, the thoracic, muscle, and skin incisions were sutured. The animals were sacrificed and the left lung tissue was collected 6h after reperfusion. The tissues were rapidly frozen in liquid nitrogen and subsequently stored at −80°C until further analysis.

Cell culture and oxygen-glucose deprivation and reoxygenation (OGD/R) model

Mouse mononuclear macrophage leukemia cells (RAW264.7 cells) were purchased from Procell Life Science & Technology Co, Ltd (Wuhan, China). The cells were cultured in Dulbecco's modified Eagle's medium (DMEM, Gibco) containing 10% fetal bovine serum (FBS; Gibco) and 1% penicillin-streptomycin (PS), incubated in a humidified cell incubator at 37°C and 5% carbon dioxide (CO2). The compound TD139 exhibits high specificity and cell-permeability as an inhibitor of Gal3. After pretreatment with either vehicle (0.025% DMSO) or 10 μM TD139 for 4 hours, OGD/R models were established according to previously described methods,[45] and cell specimens were collected at the 6-hour mark post-OGD/R for subsequent experimentation.

METHOD DETAILS

Lung wet-to-dry ratio

Mice were sacrificed and the left lung was excised. All extra-pulmonary tissues were removed. A piece of 2mm*2mm*2mm left lung tissue was collected, weighed for wet weight, dried at 60°C for 96 hours, and reweighed for dry weight. The results were expressed as the ratio of wet weight to dry weight.

Histopathological analysis

Lung tissue specimens were immersed in 4% paraformaldehyde and fixed for 24 hours, followed by rinsing with phosphate-buffered saline (PBS) for 10 minutes. After conventional dehydration and transparent treatment, the tissues were embedded in liquid paraffin (60°C). The sections were then stained with hematoxylin and eosin and imaged at magnifications of 200x and 400x using EVOS FL autollife Technologies. Lung injury was assessed according to previously described methods.[46]

Transmission electron microscopy

Lung tissue specimens were sectioned into approximately 1mm cubes and fixed overnight in 3% glutaraldehyde, followed by a 2-hour fixation with 2% osmium tetroxide. Prior to resin embedding, the tissue underwent dehydration using a gradient concentration of acetone. The specimen was cut into ultrathin

sections with ultramicrotome and observed by H-7560 transmission electron microscope and photographed (H7560, Tokyo, Japan).

Bronchoalveolar lavage fluid (BALF) acquisition and analysis

Following sacrifice of the mice, the right main bronchus was ligated at the bronchial bifurcation and 1.0 mL precooled PBS was slowly instilled into the left lung via tracheal tube for lavage. The collected BALF was centrifuged at 1500 r/min at 4°C for 10 min, and the resulting supernatant was stored at −80°C for subsequent experimental analysis.

Enzyme-linked immunosorbent assay (ELISA)

The concentrations of IL-1β, TNF-α, IL-10 and Gal3 in lung tissue, BALF and serum were quantitatively determined by ELISA kits (CUSABIO TECHNOLOGY, Wuhan, China) according to the manufacturer's instructions.

Cell viability assays

Cell viability was assayed for each group of cells separately using the CCK-8 kit (Beyotime Biotechnology, Shanghai, China) according to the manufacturer's instructions.

Immunofluorescence staining

Paraffin sections were subjected to baking at 65°C for a duration of 3 hours, followed by cooling to room temperature (RT) and subsequent dewaxing and hydration procedures. The tissue sections were immersed in a citrate buffer solution (10 mM sodium citrate, pH = 6) and subjected to antigen retrieval using microwave irradiation for a total of approximately 23 minutes (8 minutes at medium power, followed by an 8-minute cooling period, and then 7 minutes at medium-low power). After antigen retrieval, the sections were allowed to cool at room temperature for 30 minutes and then incubated overnight with a diluted primary antibody at 4°C. On the second day, after being washed three times with PBS, the corresponding secondary antibody was used to incubate for 50 minutes at room temperature under dark conditions. The sections were washed with PBS to block staining and observed under fluorescence microscope (Nikon EclipseC1, Nikon). The fluorescence intensity was quantified using Image J (NIH, USA) analysis software. Following fixation in 4% paraformaldehyde overnight, the cell slides were washed and blocked with immunostaining blocker buffer before incubation with primary antibody as previously described.

Western blotting

Left lung tissues or RAW264.7 were homogenized in RIPA buffer (Solarbio, China) supplemented with a protease inhibitor cocktail (Servicebio, China) and a phosphatase inhibitor cocktail (Cell Signaling Technology, USA). The homogenates were subjected to centrifugation at 12,000 g for 20 minutes at 4°C. The resulting supernatant was collected as the total protein and its concentration was determined using a Bicinchoninic acid kit (Beyotime Biotechnology). Proteins were separated via polyacrylamide gel electrophoresis and subsequently transferred onto polyvinylidene difluoride membranes (PVDF). The membranes were then incubated with primary and secondary antibodies at the concentrations specified below, while being maintained at 4°C. The expression levels of Gal3, TREM2, M1 markers (IL-1β, TNF-α, IL-6, CCL5), and M2 markers (Arg1, IL-10, Retnla, Chil3) were measured in the left lung tissue and RAW264.7 cells. The band density was quantified using the Alpha Innotech system (BioRad) based on an enhanced chemiluminescence method.

Total RNA extraction and real-time PCR

Total RNA was extracted from lung tissue or RAW267.4 cells using RNAiso plus (Takara Bio Inc. Kusatsu, Japan). Subsequently, 1 μg of total RNA was utilized as a template for reverse transcription reaction in a 20 μl reaction system. The Prime Script™ RT kit (Takara, Japan) was employed to perform the reverse transcription reaction according to the manufacturer's instructions. Finally, comparative Ct ($2^{-\Delta\Delta Ct}$) analysis standardized by GAPDH was used to determine relative mRNA expression levels.